

# A COMPREHENSIVE ANALYTICAL CHARACTERIZATION OF GREEK LIGNITE BOTTOM ASH SAMPLES

**Andreas IORDANIDIS<sup>1\*</sup>, Argyro ASVESTA<sup>1</sup>, Ioannis KAPAGERIDIS<sup>1</sup>, Agapi VASILEIADOU<sup>1,2</sup>,  
Kyros KOIOS<sup>1</sup>, Stavros OIKONOMIDIS<sup>3</sup> and Nikolaos KANTIRANIS<sup>3</sup>**

<sup>1</sup>Department of Mineral Resources Engineering, Faculty of Engineering, University of Western Macedonia, 50100 Kozani, Greece

<sup>2</sup>Department of Environmental Engineering, Faculty of Engineering, Democritus University of Thrace, 67100 Xanthi, Greece

<sup>3</sup>School of Geology, Aristotle University of Thessaloniki, 54124 Thessaloniki, Greece

Corresponding author Email: [aiordanidis@uowm.gr](mailto:aiordanidis@uowm.gr) & [aiordanidis@yahoo.co.uk](mailto:aiordanidis@yahoo.co.uk)

*Bottom ash samples were collected from four lignite power plants of Greece. Granulometric analysis was executed and after homogenization four distinct fractions (>1.25, 0.63-1.25, 0.18-0.63, <0.18 mm) were obtained. The samples were analyzed by X-Ray Diffraction (XRD) and Energy Dispersive System (EDS), while thermogravimetry (TG/DTG) and stereomicroscope viewing were applied for the coarse fractions. Furthermore, proximate analysis (moisture, ash, volatiles, fixed carbon) was undertaken and Loss on Ignition (LOI) and calorific values were determined. The particle size distribution revealed that bottom ash satisfies the gradation criteria for concrete and geotechnical applications. The mineral composition included mainly amorphous matter, quartz, plagioclase, calcite and gehlenite and minor amounts of pyroxene, portlandite, hematite, micas etc.. The chemical analysis showed Si, Ca, Al, Mg, Fe, S as major and Ti and K as minor chemical elements, indicating high slagging and fouling potential within the thermal chambers. Based on the chemistry and mineralogy of the bottom ash samples, a potential utilization in concrete manufacturing is discussed, taking into account certain limitations. Based on LOI, proximate analysis, calorific values and TG/DTG profiles of the coarse fractions (>1.25 mm), certain differences in the characteristics of the bottom ash of the younger and the three older power plants were observed. High amounts of unburnt carbon were determined in the coarse fraction (>1.25 mm) of all plants except the younger one, indicating a problematic combustion within the chambers and a potential of reburning these coarse material in a waste to energy application.*

**Keywords:** *Lignite bottom ash, grain size distribution, mineralogy, geochemistry, thermogravimetry (TG/DTG), EDX, XRD, calorific value, proximate analysis, energy recovery*

## 1. Introduction

Bottom ash (BA) is a coal combustion by-product derived from the thermal chambers of a thermoelectric power plant and generally preserves a high proportion of unburnt carbon. Huge amounts of bottom ash are produced in coal-consuming countries worldwide [1,2]. Approximately 700,000 tones/year of bottom ash were produced in the lignite-fired power plants of Greece during the previous decades [3,4]. Bottom ash is used globally in concrete industry, road constructions, geotechnical and environmental applications, e.g. as aggregate in lightweight concrete, as fine aggregate in cement mortars, as a raw material in the cement clinker raw meal, as a soil amendment, in asphalt mixes etc.. [5-11].

In Greece, it is entirely deposited in abandoned lignite mine sites and/or in landfills. It should be noted however that due to recent political decisions, lignite production will be dismissed until the end of 2030, since the use of fossil fuels is considered highly polluting and releases greenhouse gases. Thus, the amounts of coal combustion by-products will be inevitably limited. Nevertheless, excessive quantities of bottom ash have already been dumped, since there was an intensive exploitation of lignite deposits the last fifty years.

The analytical characterization of bottom ash samples is a prerequisite in order to suggest any potential utilization. Likewise, useful information could be derived regarding the combustion parameters within the thermal chamber, which could be used in order to improve the energy efficiency of the power plant. The potential utilization of the relatively high contents of unburnt carbon, in an attempt to evaluate their energy recovery, is also an asset. X-Ray Fluorescence (XRF), X-Ray Energy Dispersive (EDS) and X-Ray Diffraction (XRD) are the state of the art techniques for chemical and mineralogical studies of such material [7,12,13]. Thermo-analytical methods may also provide a rapid, cost-effective assessment of the fuel quality or mineral composition of several materials and thermogravimetry (TG) is one of the most widespread technique for an initial evaluation of such materials [14-16].

The assessment of the morphological, physicochemical, mineralogical and thermal characteristics of selected Greek, lignite bottom ash samples is the aim of the present study, in order to discuss their potential applications and assess the efficiency of the thermoelectric power stations.

## 2. Material and Methods

Bottom ash (BA) samples were collected from four lignite power plants, i.e. Agios Dimitrios (DIM), Kardias (KAR), Meliti (MLT) (Western Macedonia, northern Greece) and Megalopoli (MGL) (Peloponnese, southern Greece). Kardias's thermoelectric plant was founded in 1975 and has a capacity of 1200 MW, while Agios Dimitrios's and Megalopoli's plants, with a capacity of 1600 MW and 850 MW respectively, were founded in 1980's and the newest Meliti's power plant was founded in 2003 and has a capacity of 330 MW.

All samples were dried in oven at 100 °C for 24 hours. Dry sieving was applied in order to obtain the particle size distribution. Four distinct fractions (>1.25 mm, 0.63-1.25 mm, 0.18-0.63 mm, <0.18 mm) of each sample were obtained after homogenization and ground for further analyses. Moreover, a Euromex stereo-microscope coupled to CMEX-1 digital camera and the Image Focus software was employed in order to study the microscopic features of the coarse fraction (>1.25 mm) of all samples,

before grinding. Proximate analysis (moisture, ash, volatile matter and fixed carbon) and Loss on Ignition (LOI) determination were performed with the LECO TGA 701 device, based on the ASTM D 5142-09 ASTM D 7348-13 standards respectively [17,18]. The determination of the calorific value was made with the LECO AC-500 isoperibol bomb calorimeter, using the ASTM D 5865-13 standard [19]. Samples were also analyzed by thermogravimetry (TG/DTG), using the LECO TGA701 apparatus, according to the following procedure: approximately 500 mg of each sample was heated from room temperature (25 °C) up to 1000 °C, with a heating ramp of 10 °C/min, under air atmosphere, with a flow rate of 3.5 l/min. For the X-ray diffraction (XRD), a Phillips PW1710 diffractometer was used with a CuK $\alpha$  radiation source. The XRD patterns were obtained by step scanning from 3° to 63° in scan speed 0.020° 2 $\theta$ /s. The Oxford INCA 250 energy dispersive spectrometer (EDS) coupled to the JEOL JSM-840A Scanning Electron Microscope was used for the chemical analysis.

### 3. Results and Discussion

#### 3.1 Granulometry and Minerochemical composition

The particle size distribution of the analyzed BA samples is shown in Figure 1. It is evident that coarse fractions with a size greater than 1.60 mm prevail for MLT sample, while in the other samples (DIM, KAR and MGL), the fractions with a size ranging between 0.18 and 1.25 mm have the highest proportions. In particular, 43 wt% of MLT sample exhibit a size >2.5 mm, whereas the most abundant grain size fraction in DIM, KAR and MGL samples is below 0.63 mm and above 0.18 mm, with a percentage of 45 wt%, 47 wt% and 59 wt%, respectively. It is well known that the mechanical and durability properties of concretes depend on the grain size distribution of BA [6,8,10]. Since the grain size of BA particles of this study resembles the grain size of fine aggregates with low percentage of silt-clay, it could be concluded that BA can successfully replace the fine aggregates in the manufacturing of concrete [9,10]. Moreover, the particle size distribution satisfies the gradation criteria for utilization as strengthened/reinforced soil (backfill material) [8].

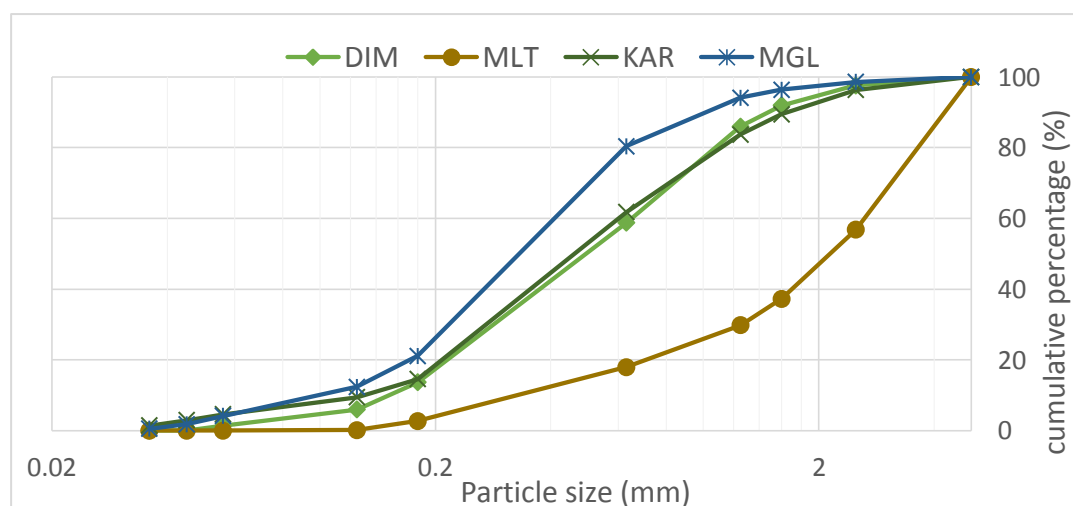


**Figure 1. Particle size distribution (mm) of the four analyzed bottom ash samples. (DIM: Agios Dimitrios, MLT: Meliti, KAR: Kardìa, MGL: Megalopoli)**

**Table 1. Chemical composition (major oxides, wt%), Slagging (Rs), Fouling (Fu) and Slag viscosity (Sr) indices of all fractions of the bottom ash samples (DIM: Agios Dimitrios, MLT: Meliti, KAR: Kardia, MGL: Megalopoli).**

SAMPLES	MgO	Al <sub>2</sub> O <sub>3</sub>	SiO <sub>2</sub>	SO <sub>3</sub>	CaO	Fe <sub>2</sub> O <sub>3</sub>	TiO <sub>2</sub>	K <sub>2</sub> O	Rs	Fu	Sr
DIM>1.25	3.07	14.62	28.77	7.68	39.33	6.53	-	-	2.2553	0	37.0270
DIM>0.63	3.48	14.70	38.51	2.79	32.67	5.13	-	2.72	0.6946	2.2492	48.2641
DIM>0.18	3.96	14.96	30.12	9.05	32.05	7.09	-	1.44	2.7565	1.4227	41.1363
DIM<0.18	4.27	11.94	26.96	7.20	43.74	3.78	-	2.11	2.7573	2.9236	34.2349
MLT>1.25	4.21	19.52	46.43	5.94	12.70	8.41	2.31	0.49	0.8583	0.1852	64.7108
MLT>0.63	2.98	22.36	44.35	6.10	16.60	5.40	-	2.22	0.7706	0.9051	63.9694
MLT>0.18	4.14	12.91	27.58	16.13	39.24	-	-	-	4.6176	0	38.8669
MLT<0.18	4.62	18.15	32.03	8.16	33.41	3.63	-	-	2.0589	0	43.4658
KAR>1.25	5.86	10.97	28.97	9.13	39.35	5.12	-	-	2.6013	0	36.2578
KAR>0.63	4.52	13.53	32.24	6.73	35.70	4.74	-	2.55	1.8891	2.6469	41.7616
KAR>0.18	3.29	17.39	37.49	5.46	27.18	6.41	-	-	1.1625	0	50.4101
KAR<0.18	3.97	12.18	27.03	5.30	41.79	5.34	-	1.04	1.9148	1.3829	34.5961
MGL>1.25	3.47	11.94	32.44	21.33	20.32	7.10	1.28	2.10	4.3466	1.5162	51.2237
MGL>0.63	3.26	16.33	45.30	11.38	15.73	6.91	-	1.08	1.6810	0.4727	63.6235
MGL>0.18	2.61	18.13	41.16	6.61	16.25	12.61	-	2.63	1.3918	1.5126	56.6707
MGL<0.18	4.11	17.34	41.76	3.67	17.99	12.16	1.03	1.94	0.7525	1.1679	54.9329
<b>Average</b>	<b>3.86</b>	<b>15.44</b>	<b>35.07</b>	<b>8.29</b>	<b>29.04</b>	<b>6.69</b>	<b>1.54</b>	<b>1.85</b>	<b>2.0318</b>	<b>1.0241</b>	<b>47.5720</b>

The chemical composition of BA samples is shown in Table 1. The analysis of major oxides ascertains a differentiation in the chemical composition of MLT sample. Thus, while DIM, KAR and MGL samples are composed of elevated contents of CaO were found for all samples, ranging between 12.70 wt% (MLT>1.25) and 43.74 wt% (DIM<0.18), while the MLT>1.25 sample reveal the highest contents of SiO<sub>2</sub> (46.43 wt%), and the range of SiO<sub>2</sub> content in all the other samples is between 26.96 wt% (DIM<0.18) and 45.30 wt% (MGL>0.63). The MgO content ranges between 2.61 and 5.86 wt%, Al<sub>2</sub>O<sub>3</sub> between 10.97 and 19.52 wt% and Fe<sub>2</sub>O<sub>3</sub> between 5.12 and 8.41 wt%. The SO<sub>3</sub> amounts are rather high, especially for the coarse fractions of MGL samples (21.33 wt%), a fact that is related to the high sulphur contents of the Megalopoli lignite deposits. This fact inhibits a potential application in concrete industry, since the high Sulphur contents may cause loss in the compressive strength and increase drying shrinkage in concrete applications [2]. Minor amounts of TiO<sub>2</sub> (up to 2.31 wt%) and K<sub>2</sub>O (up to 2.72 wt%) were also found in some samples, while Na<sub>2</sub>O was absent. The high amounts of silica and alumina contents, apparently in a glassy-amorphous state, are indicative for pozzolanic properties, while the high calcium contents suggest hydraulic/self-cementing properties [2,8-11]. Regarding potential hazardous heavy metals, low amounts of copper (<2 wt%) were only detected in the fine fractions (<0.63mm) of KAR sample (not included in Table 1). Therefore, the possibility of leaching of potential toxic heavy metals in the environment should be investigated by employing chemometric methodologies suitable for trace element identification [2,13].

The calculation of the slagging (Rs), fouling (Fu) and slag viscosity (Sr) indices is based on Yang et al. (and references therein) [20], according to the following four equations:

$$\frac{B}{A} = \frac{Fe_2O_3 + CaO + MgO + Na_2O + K_2O}{SiO_2 + Al_2O_3 + TiO_2} \quad (1)$$

$$R_s = \frac{B}{A} \times S \quad (2)$$

$$F_u = \frac{B}{A} \times (K_2O + Na_2O) \quad (3)$$

$$S_r = \frac{SiO_2 \times 100}{SiO_2 + Fe_2O_3 + CaO + MgO} \quad (4)$$

**Table 2. Mineralogical composition (wt%) of all fractions of the bottom ash samples (DIM: Agios Dimitrios, MLT: Meliti, KAR: Kardia, MGL: Megalopoli). [Am=Amorphous, Qz=Quartz, Ca=Calcite, Pl=Plagioclase, Ge=Gehlenite, Mi=Micas, Py=Pyroxene, Po=Portlandite, Hm=Hematite, Kf=K-feldspar, Ma=Maghemite, Do=Dolomite, Cr=Cristobalite, Mg=Magnetite, La=Larnite]**

SAMPLES	Am	Qz	Ca	Pl	Ge	Mi	Py	Po	Hm	Kf	Ma	Do	Cr	Mg	La
DIM>1.25	27	10	60	-	-	2	-	-	-	-	-	-	1	-	-
DIM>0.63	36	27	33	2	1	1	-	-	-	-	-	-	-	-	-
DIM>0.18	40	33	15	5	7	-	-	-	-	-	-	-	-	-	-
DIM<0.18	32	18	29	4	11	-	-	-	-	-	-	-	-	3	3
MLT>1.25	33	22	15	16	-	-	8	-	6	-	-	-	-	-	-
MLT>0.63	41	15	14	9	4	-	-	11	-	6	-	-	-	-	-
MLT>0.18	37	23	16	6	4	-	-	14	-	-	-	-	-	-	-
MLT<0.18	43	11	20	5	6	1	-	14	-	-	-	-	-	-	-
KAR>1.25	30	14	33	4	5	2	8	-	4	-	-	-	-	-	-
KAR>0.63	29	18	33	7	-	2	-	-	-	8	-	3	-	-	-
KAR>0.18	26	34	19	15	5	1	-	-	-	-	-	-	-	-	-
KAR<0.18	35	16	34	5	8	-	-	2	-	-	-	-	-	-	-
MGL>1.25	27	30	27	2	-	3	-	-	9	-	-	-	-	-	-
MGL>0.63	33	39	12	7	-	1	8	-	-	-	-	-	-	-	-
MGL>0.18	36	23	5	9	7	1	6	-	-	-	13	-	-	-	-
MGL<0.18	38	21	7	7	8	-	6	-	-	-	13	-	-	-	-

The results are shown in Table 1. The average value of slagging ( $R_s$ ) index was 2.0318, while fouling ( $F_u$ ) and slag viscosity ( $S_r$ ) indices had values of 1.0241 and 47.5720 respectively. Since  $R_s$  values between 2 and 2.6,  $F_u$  values between 0.6 and 40 and  $S_r$  values <65 are related to high slagging, fouling and slag viscosity potential [20], the BA samples of the present study could be considered harmful for the thermal chambers of the lignite-fired power plants.

The semi-quantitative mineralogical results of the analyzed BA samples are shown in Table 2. It is evident that amorphous matter is prevailing in all samples, with concentrations ranging between 26 and 43 wt%. This amorphous material is attributed either to carbonaceous matter or to the inorganic fused ash material [2,21]. The presence of unburnt carbon has frequently been considered beneficial for an overall improvement in concrete manufacturing [9]. Calcite [ $CaCO_3$ ] was the most dominant mineral, with concentrations ranging from 5% to 60 wt%. Quartz [ $SiO_2$ ] was the next most common mineral, showing contents of 10-39 wt%. Plagioclase [anorthite,  $CaAl_2Si_2O_8$ ], ranging between 2 and 16 wt% and Gehlenite [ $Ca_2Al_2SiO_7$ ], ranging between 1 and 11 wt% were the additional main crystalline mineral phases that were identified in all samples. Substantial amounts of Portlandite [ $Ca(OH)_2$ ] were found mainly in MLT samples (2-14 wt%), Pyroxene [Augite,  $(Ca,Na)(Mg,Fe,Al,Ti)(Si,Al)_2O_6$ ] mainly in MGL samples (6-8 wt%) and iron-rich phases, such as Hematite [ $Fe_2O_3$ ] (4-9 wt%), Magnetite [ $Fe_3O_4$ ] (3 wt%) and Maghemite [ $\gamma-Fe_2O_3$ ] (13 wt%) in a few samples. Micas [muscovite,  $KAl_3Si_3O_{10}(OH,F)_2$ ] were also identified in very low amounts ( $\leq 3$  wt%) in several samples, while Dolomite [ $CaMg(CO_3)_2$ ], K-Feldspar [ $KAlSi_3O_8$ ], Cristobalite [ $SiO_2$ ] and

Larnite [Ca<sub>2</sub>SiO<sub>4</sub>] were also sporadically assigned with concentrations up to 3 wt%. The prevalence of amorphous phases, along with the presence of aluminosilicate minerals, portlandite and calcite suggest a beneficial pozzolanic activity in concrete manufacturing, although certain upper limits do occur for definite concrete applications [1,2]. Therefore, a careful grinding and processing of the BA material may provide BA categories adapted for specific applications.

### 3.2 Proximate analysis and Thermal characteristics

Proximate analysis, Loss on Ignition (LOI), Total Weight Loss (based on TG analysis) and gross calorific values of all samples are shown in Table 3. The ash content is generally high, as it is anticipated for bottom ash material. However, the coarse fraction (>1.25 mm) samples of the DIM, KAR and MGL bottom ash reveal rather low ash contents (down to 36.90 wt%), a fact that implies high proportions of unburnt carbon in their composition. Nevertheless, this is not the case for MLT sample. The range of volatile matter (VM) is between 6.01 wt% (MGL>0.18) and 37.51 wt% (DIM>1.25). Once more, MLT samples present the lowest VM values, while the coarse fractions of the other three BA samples retain the highest VM contents. Fixed carbon (FC) content ranges from 0.05 wt% to 21.64 wt%. In general, the fine fractions (<0.63 mm) present low FC values, except MLT samples, which differentiate from this trend. LOI values range between 6.88 wt% (MGL>0.18) and 62.17 wt% (KAR>1.25), resembling the trend of VM content. The exceptional high LOI values limit the use of a BA in cementitious materials due to possible future durability problems and may lead to discoloration, weak air entrainment, segregation and low compressive strength [2,6]. It should be noted however that LOI values are usually determined by XRF methodology and not by thermal techniques, which is the case in our study. Therefore, based solely on LOI contents, no secure conclusions could be derived regarding the application of BA in concrete materials. Accordingly, the total weight loss values range from 7.20 wt% (MGL>0.18) to 64.24 wt% (KAR>1.25). Finally, the gross calorific value (GCV) ranges between 0.43 MJ/kg (MGL>0.18) and 12.71 MJ/kg (KAR>1.25).

**Table 3. Proximate analysis (moisture, ash, volatile matter, fixed carbon), Loss on Ignition (LOI), Weight Loss (based on TG profile) and gross calorific values (GCV) of all fractions of the bottom ash samples (DIM: Agios Dimitrios, MLT: Meliti, KAR: Kardia, MGL: Megalopoli). All values are in wt%, except GCV.**

SAMPLES	Moisture	Ash	Volatile Matter	Fixed Carbon	LOI	Total Weight Loss	GCV (MJ/kg)
DIM>1.25	6.83	41.77	37.51	13.89	58.22	58.11	9.82
DIM>0.63	4.11	70.13	19.03	6.73	30.26	30.31	3.31
DIM>0.18	3.40	78.75	15.05	2.80	20.99	20.48	1.85
DIM<0.18	4.27	72.68	23.00	0.05	27.88	28.02	2.28
MLT>1.25	2.35	81.92	7.29	8.44	17.74	18.23	3.05
MLT>0.63	2.38	82.31	10.05	5.26	17.24	17.76	2.65
MLT>0.18	2.78	78.80	12.72	5.70	21.36	21.88	3.72
MLT<0.18	4.62	68.81	16.84	9.73	30.35	31.13	5.64
KAR>1.25	7.52	36.90	33.94	21.64	62.17	64.24	12.71
KAR>0.63	4.28	61.35	21.51	12.86	39.04	39.24	7.16
KAR>0.18	2.60	78.84	13.79	4.77	19.91	18.36	2.99
KAR<0.18	3.83	67.92	26.92	1.33	31.62	31.81	5.38
MGL>1.25	8.74	46.01	32.98	12.27	53.87	53.66	10.26
MGL>0.63	4.42	74.00	14.39	7.19	26.00	25.72	4.99
MGL>0.18	1.26	92.45	6.01	0.28	6.88	7.20	0.43

MGL<0.18 | 2.05 87.79 9.67 0.49 10.79 9.06 1.17

Consequently, Meliti sample (MLT), showing high ash content (up to 81.92 wt%), low volatile matter (down to 7.29 wt%), fixed carbon (down to 5.26 wt%), LOI (down to 17.24 wt%), total weight loss (down to 17.76 wt%) and gross calorific (down to 2.65 MJ/kg) values, clearly differs from the other samples (DIM, KAR and MGL), which have lower ash contents (down to 36.90 wt%) and higher volatile matter (up to 37.51 wt%), fixed carbon (up to 21.64 wt%), LOI (up to 62.17 wt%), total weight loss (up to 64.24 wt%) and GCV (up to 12.71 MJ/kg) values. It is evident from the proximate analysis and the LOI, total weight loss and calorific value determinations that the coarse fraction (>1.25 mm) of three BA samples (DIM, KAR and MGL) have adequate combustible matter and can be re-utilized for energy production. Therefore, their combustion characteristics are further discussed in the next section. Besides, a problematic combustion is inferred for the older Agios Dimitrios (DIM), Kardia (KAR) and Megalopoli (MGL) power plants, while the characteristics of MLT samples indicate a better combustion performance within the younger Meliti power plant.

The correlation of the proximate analysis data with the mineralogical and chemical composition provided significant information. For example, the regression plot between calcite and volatile matter contents ( $R^2=0.74$ ) indicates that a great amount of volatiles is attributed to the calcite decomposition and not the organic material itself, while the regression of ash *versus* amorphous matter ( $R^2=0.32$ ) indicates a medium positive correlation and therefore provides evidence for the existence of both organic and inorganic matter in the amorphous phases found by XRD (Fig. 2). MLT samples exhibit indeed a clear differentiation in their characteristics when compared to the other three BA samples and thus it is noticeable that when MLT samples are excluded from the calculations, the above mentioned correlations are becoming stronger.

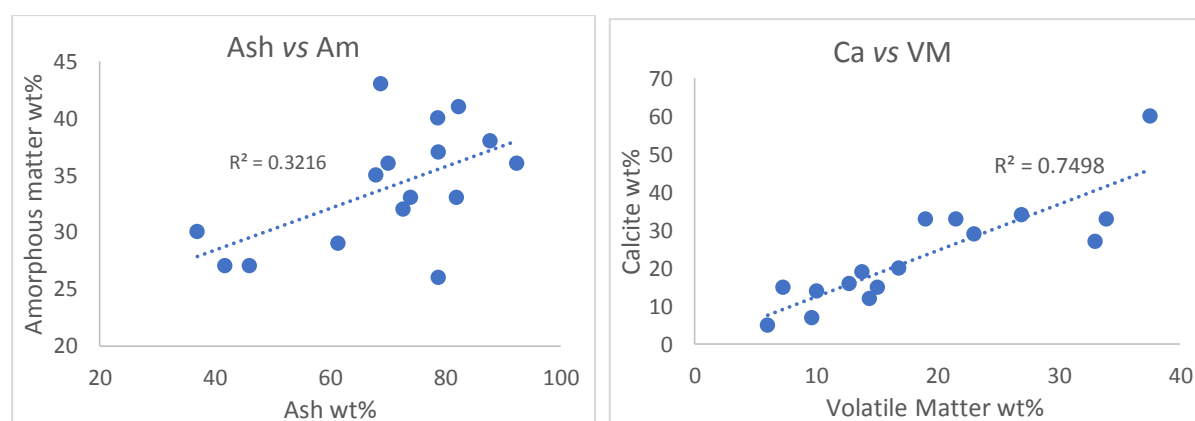


**Figure 2. Regression plots of Ash *versus* Amorphous Matter (Am) contents (left) and Calcite *versus* Volatile Matter (VM) contents (right) for all the analyzed bottom ash samples.**

### 3.3 TG/DTG profiles of the coarse fractions (>1.25mm)

The stereo-microscope viewing of the coarse fractions (i.e. >2.5 mm, 1.6-2.5 mm and 1.25-1.6 mm) of all BA samples revealed char particles of several dimensions and shapes, showing a black or brown colour, a porous/vesicular structure and a spherical or elongated morphology (Figure 3). Additionally, inorganic (some partially fused) particles of several dimensions, having round, angular or irregular

shapes and showing mostly a grey colour, have also been observed (Figure 3).

Figure 4 illustrates the compiled TG/DTG profiles of the coarse fraction (>1.25 mm) of the four BA samples of this study. Three distinctive regions are shown in these profiles. The first region on DTG curves (<150 °C) corresponds to the moisture loss. The second region (200 °C – 700 °C) is due to oxidation and removal of volatile matter and the oxidation of the remaining char [16,21]. Moreover, there are peaks in rather high temperature (>800 °C), which are probably attributed to calcite decomposition or to transformation of the inorganic matter to neo-minerals at such high temperatures. [15,16].

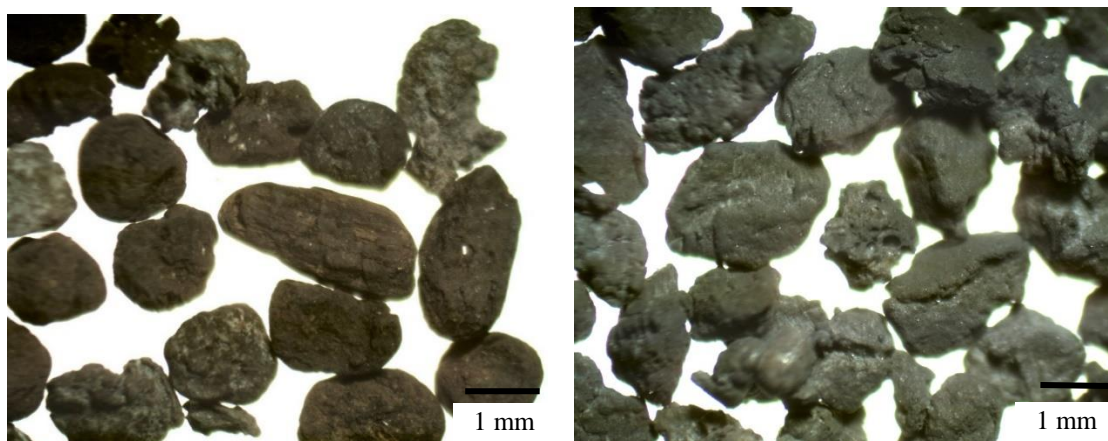


**Figure 3. Microphotographs of characteristic aggregates of coarse particles (>1.25mm) from Megalopoli (MGL) [left] and Meliti (MLT) [right] bottom ash samples.**

The combustion characteristics of the coarse fraction (>1.25 mm) of all the analyzed samples are illustrated in Table 4. Thermal parameters such as ignition temperature ( $T_i$ ), maximum rate of weight loss ( $R_{max}$ ), peak and burnout temperatures ( $T_{max}$ ,  $T_b$ ) were determined from the thermogravimetry (TG/DTG) profiles. Definitions are explained by Vamvuka et al. [14,15] and in our previous work [16]. The total weight loss, as determined by the TG methodology (Table 3), varies between 18.23% (MLT) and 64.24% (KAR). The ignition temperature ( $T_i$ ) ranges between 204 °C (MGL) and 295 °C (MLT). The burnout temperature ( $T_b$ ) displays values between 849 °C (MLT) and 970 °C (KAR), while the peak temperature  $T_{max}$  varies between 576 °C (MLT) and 903 °C (DIM). The maximum rate of weight loss appears with values up to 2%/min (DIM sample) and mostly occurs in the temperature range of 730 °C – 950 °C (Figure 4). However, MLT sample reveals a rather low maximum rate of weight loss (0.4 %/min) and in a different temperature range (330 °C – 770 °C). It is evident that the sample with enhanced value of FC (MGL) generally ignite at lower temperatures and these lower  $T_i$  values usually correspond to better combustibility [15,16]. A clear association of the maximum weight loss rate ( $R_{max}$ ) with the volatile mater (VM) content is also found, i.e. samples with high volatile matter content, such as DIM exhibit high  $R_{max}$ .

**Table 4. Combustion characteristics of the coarse fractions (>1.25mm) of the analyzed bottom ash samples (DIM: Agios Dimitrios, MLT: Meliti, KAR: Kardia, MGL: Megalopoli).**

SAMPLES	$T_i$ (°C)	$T_b$ (°C)	$T_{max}$ (°C)	$R_{max}$ (%/min)
DIM>1.25	228	910	903	2.00
MLT>1.25	295	849	576	0.40



KAR>1.25	220	970	858	1.48
MGL>1.25	204	955	881	1.06

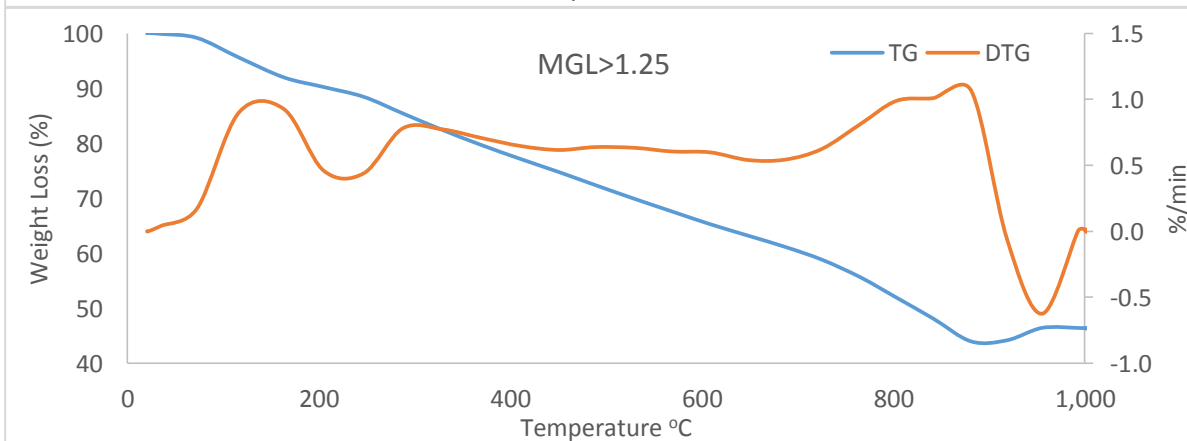
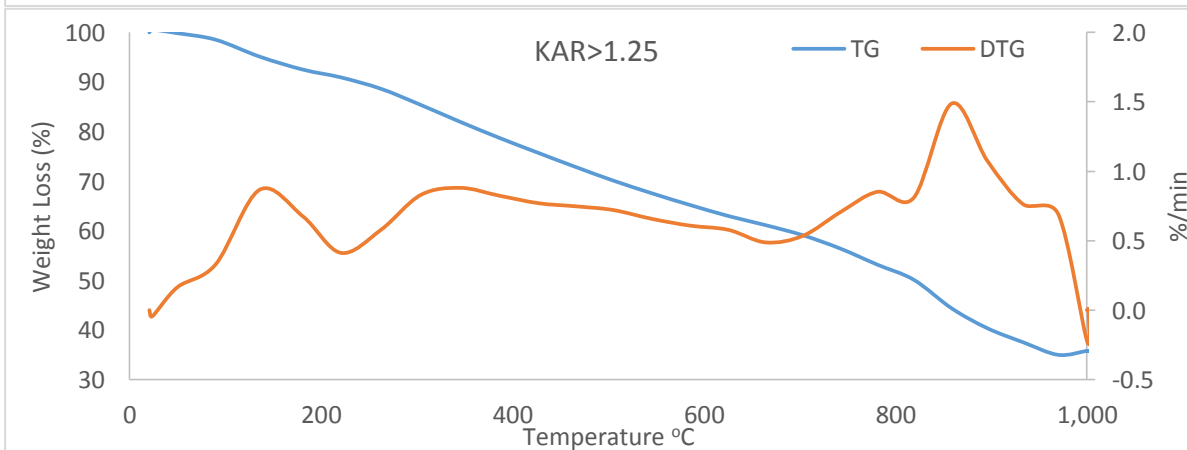
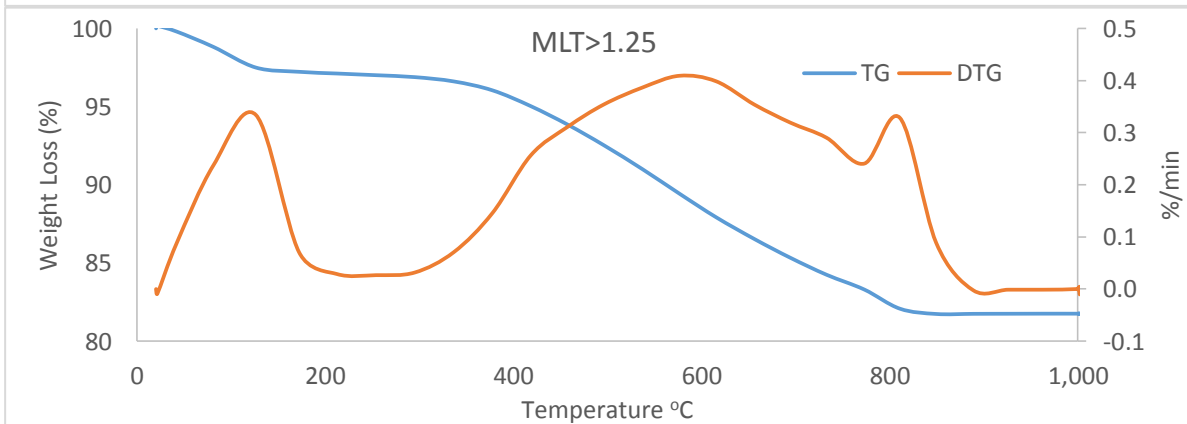
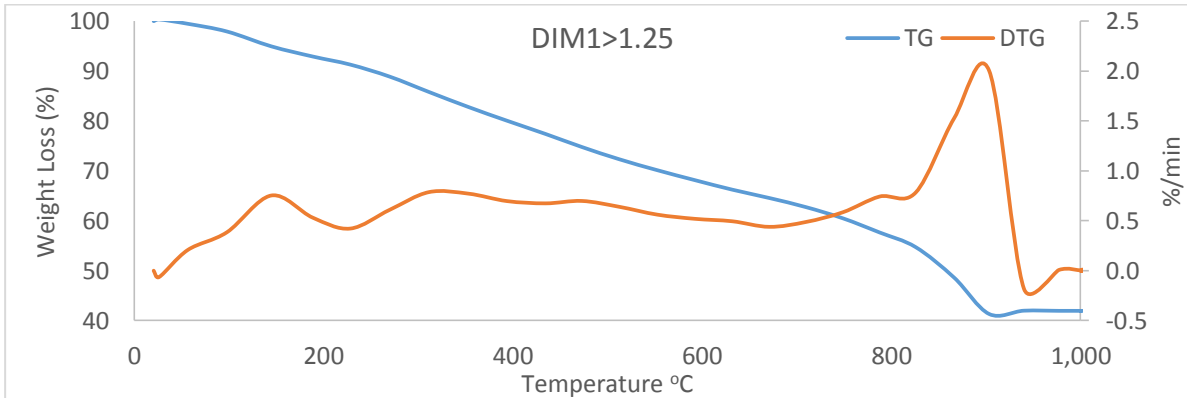


**Figure 4. TG/DTG profiles of the coarse fractions (>1.25mm) of the analyzed bottom ash samples (DIM: Agios Dimitrios, MLT: Meliti, KAR: Kardia, MGL: Megalopoli).**

Overall, the determined combustion characteristics (ignition temperature, maximum rate of weight loss, peak and burnout temperatures) indicate the high potential of the coarse particles of BA samples for energy production (except MLT sample). Therefore, the reburning of the carbon-rich coarse fraction of bottom ash, which could be easily recovered after careful screening, is an attractive option regarding the beneficial utilization of Greek bottom ash [3,12,22,23]. This combustible material could be considered as a renewable, low cost energy source, which can be co-fired with miscellaneous solid wastes and/or coal, minimizing the coal waste load in general and reducing the dependency on fossil fuels [24].

#### **4. Conclusions**

Several fractions of bottom ash samples from four Greek lignite-fired power plants were analyzed in this study. Definite differences in the characteristics of the bottom ash samples collected from the younger Meliti power plant comparing to the older (>30 years) Agios Dimitrios, Kardia and Megalopoli plants were found. The thermal characteristics (proximate, LOI, GCV, TG/DTG) and the chemical (EDX) and mineralogical (XRD) composition of the analyzed BA samples provided important information regarding the efficiency of the power plants (unburnt carbon, slagging and fouling indices) as well as the potential utilization of this lignite combustion by-product.

The analytical results witness for the poor combustion in the older power plants, comparing to the higher efficiency and the improved coal combustion technologies in the younger power plant. In particular, high amounts of unburnt carbon (enhanced values of fixed carbon, LOI and weight loss) were determined in the samples from Agios Dimitrios, Kardia and Megalopoli plants, while Meliti's samples revealed low amounts of carbonaceous matter. The results imply a problematic combustion and a low energy efficiency for the older thermal plants compared to the higher efficiency of Meliti's plant. High slagging and fouling potential were calculated based on the abundance of specific chemical elements, a fact that provokes inevitable detrimental effects in the thermal chambers of the thermoelectric stations.

The presence of glassy/amorphous aluminosilicate phases in the ingredients of the BA samples along with their calcareous nature suggested a possible utilization in concrete and other geotechnical applications, taking into the account specific limitations. A careful processing of the BA could provide material that satisfies specific geotechnical needs.

#### **Acknowledgment**

The authors would like to thank the University of Western Macedonia for the financial support of this research project (RESCOM 80288).

#### **Nomenclature**

Am	Amorphous	MGL	Megalopoli power plant
BA	Bottom Ash	Mi	Micas
Ca	Calcite	MLT	Meliti power plant
Cr	Cristobalite	Pl	Plagioclase
DIM	Agios Dimitrios power plant	Po	Portlandite

Do	Dolomite	Qz	Quartz
EDS	X-Ray Energy Dispersive System	R <sub>max</sub>	maximum rate of weight loss (%/min)
FC	Fixed carbon (wt%)	Rs	Slagging index
Fu	Fouling index	Sr	Slag viscosity index
Ge	Gehlenite	T <sub>b</sub>	burnout temperature (°C)
GCV	Gross Calorific Value (MJ/kg)	T <sub>i</sub>	ignition temperature (°C)
Hm	Hematite	T <sub>max</sub>	peak temperature at the maximum rate of weight loss (°C)
KAR	Kardia power plant	VM	Volatile Matter (wt%)
Kf	K-feldspar	wt%	weight percentage
Ma	Maghemite	XRD	X-Ray Diffraction
Mg	Magnetite		

## References

- [1] Muthusamy, K., *et al.*, Coal bottom ash as sand replacement in concrete: A review, *Construction and Building Materials*, 236 (2020), 117507.
- [2] Singh, N., *et al.*, Reviewing the role of coal bottom ash as an alternative of cement, *Construction and Building Materials*, 233 (2020), 117276.
- [3] Margetis, S.P., Study of lignite recovery from bottom ash by gravimetric technique, MSc thesis, University of Crete, Chania, Greece, 2014 [in Greek]
- [4] Megalovasilis, P., *et al.*, Mineralogy, geochemistry and leachability of ashes produced after lignite combustion in Amyntaio Power Station, northern Greece, *Energy Sources, Part A: Recovery, Utilization, and Environmental Effects*, 38:10 (2016), pp. 1385-1392.
- [5] Lin, C.Y., Yang, D.H., Removal of pollutants from wastewater by coal bottom ash, *Journal of Environmental Science and Health - Part A Toxic/Hazardous Substances and Environmental Engineering*, 37 (8) (2002), pp. 1509-1522.
- [6] Menéndez, E., *et al.*, Characterization of bottom ashes from coal pulverized power plants to determine their potential use feasibility, *Boletín de la Sociedad Española de Cerámica y Vidrio*, 52 (2014), pp. 296-304.
- [7] Jayaranjan, M.L.D., *et al.*, Reuse options for coal fired power plant bottom ash and fly ash, *Reviews in Environmental Science and Biotechnology*, 13 (4) (2014), pp. 467-486.
- [8] Singh, N., *et al.*, Influence of coal bottom ash as fine aggregates replacement on various properties of concretes: A review, *Resources, Conservation and Recycling*, 138 (2018), pp. 257-271.
- [9] Pant, A., *et al.*, Coal combustion residue as structural fill material for reinforced soil structures, *Journal of Cleaner Production*, 232 (2019), pp. 417-426.
- [10] Singh, N., *et al.*, Utilization of coal bottom ash in recycled concrete aggregates based self compacting concrete blended with metakaolin, *Resources, Conservation and Recycling*, 144 (2019), pp. 240-251.
- [11] Pliatsikas, I., *et al.*, Valorization of demolition ceramic wastes and lignite bottom ash for the production of ternary blended cements, *Construction and Building Materials*, 229 (2019), 116879.
- [12] Kantiranis, N., *et al.*, Mineralogy and organic matter content of bottom ash samples from Agios Dimitrios power plant, Greece, *Bulletin of the Geological Society of Greece*, 36(1) (2004), pp. 320-326.
- [13] Tiwari, M., *et al.*, Elemental characterization of coal, fly ash, and bottom ash using an energy dispersive X-ray fluorescence technique, *Applied Radiation and Isotopes*, 90 (2014), pp. 53-57.
- [14] Vamvuka, D., Sfakiotakis, S., Combustion behaviour of biomass fuels and their blends with lignite, *Thermochimica Acta*, 526 (2011), pp. 192-199.
- [15] Vamvuka, D., *et al.*, Evaluation of urban wastes as promising co-fuels for energy production – A TG/MS study, *Fuel*, 147 (2015), pp. 170-183.

- [16] Iordanidis, A., *et al.*, Combustion behaviour of different types of solid wastes and their blends with lignite, *Thermal Science*, 22 (2) (2018), pp. 1077-1088.
- [17] ASTM D 5142-09, Standard Test Methods for Proximate Analysis of the Analysis Sample of Coal and Coke by Instrumental Procedures, ASTM International, West Conshohocken, PA, 2009.
- [18] ASTM D 7348-13, Standard Test Methods for Loss on Ignition (LOI) of Solid Combustion Residues, West Conshohocken, PA, 2013
- [19] ASTM D 5865-13, Standard Test Method for Gross Calorific Value of Coal and Coke, ASTM International, West Conshohocken, PA, 2013.
- [20] Yang, M., *et al.*, Lowering ash slagging and fouling tendency of high-alkali coal by hydrothermal pretreatment, *International Journal of Mining Science and Technology*, 29 (3) (2019), pp. 521-525.
- [21] Iordanidis, A., *et al.*, Application of TG-DTA to the study of Amynteon lignites, Northern Greece, *Thermochimica Acta*, 371 (2001), pp. 137-141.
- [22] Uçurum, M., *et al.*, A Study on Characterization and Use of Flotation to Separate Unburned Carbon in Bottom Ash from Çayirhan Power Plant, *Energy Sources, Part A: Recovery, Utilization, and Environmental Effects*, 33:6 (2011), pp. 562-574.
- [23] Ramme, B.W., Tharaniyil, M.P., *Coal Combustion Products Utilization Handbook* (2013), We Energies editions (3<sup>rd</sup> ed.), pp. 438.
- [24] Magdziarz, A., Wilk, M., Thermogravimetric study of biomass, sewage sludge and coal combustion, *Energy Conversion and Management*, 75 (2013), pp. 425-430.

Submitted: 06.06.2020.

Revised: 25.08.2020.

Accepted: 03.09.2020.